



## UWS Academic Portal

### **The role of nanoparticle format and route of administration on self-amplifying mRNA vaccine potency**

Anderluzzi, Giulia; Lou, Gustavo; Woods, Stuart; Schmidt, Signe Tandrup; Gallorini, Simona; Brazzoli, Michela; Johnson, Russell; Roberts, Craig W.; O'Hagan, Derek T.; Baudner, Barbara C.; Perrie, Yvonne

*Published in:*  
Journal of Controlled Release

*DOI:*  
[10.1016/j.jconrel.2021.12.008](https://doi.org/10.1016/j.jconrel.2021.12.008)

Published: 20/01/2022

*Document Version*  
Peer reviewed version

[Link to publication on the UWS Academic Portal](#)

*Citation for published version (APA):*

Anderluzzi, G., Lou, G., Woods, S., Schmidt, S. T., Gallorini, S., Brazzoli, M., Johnson, R., Roberts, C. W., O'Hagan, D. T., Baudner, B. C., & Perrie, Y. (2022). The role of nanoparticle format and route of administration on self-amplifying mRNA vaccine potency. *Journal of Controlled Release*, *342*, 388-399. <https://doi.org/10.1016/j.jconrel.2021.12.008>

**General rights**

Copyright and moral rights for the publications made accessible in the UWS Academic Portal are retained by the authors and/or other copyright owners and it is a condition of accessing publications that users recognise and abide by the legal requirements associated with these rights.

**Take down policy**

If you believe that this document breaches copyright please contact [pure@uws.ac.uk](mailto:pure@uws.ac.uk) providing details, and we will remove access to the work immediately and investigate your claim.

1 **Title:** The role of nanoparticle format and route of administration on self-amplifying  
2 mRNA vaccine potency

3

4 **Authors:** Giulia Anderluzzi<sup>1,2†</sup>, Gustavo Lou<sup>1,2†</sup>, Stuart Woods<sup>1</sup>, Signe Tandrup Schmidt<sup>1,4</sup>, Simona  
5 Gallorini<sup>2</sup>, Michela Brazzoli<sup>2</sup>, Russell Johnson<sup>3</sup>, Craig W. Roberts<sup>1</sup>, Derek T. O’Hagan<sup>3</sup>, Barbara  
6 C. Baudner<sup>2\*</sup> and Yvonne Perrie<sup>1\*</sup>

7

8 <sup>1</sup>Strathclyde Institute of Pharmacy and Biomedical Sciences, University of Strathclyde, 161  
9 Cathedral St., Glasgow, Scotland. G4 0RE

10 <sup>2</sup>GSK, Siena, Italy.

11 <sup>3</sup>GSK, Rockville, MD 9911, USA.

12 <sup>4</sup>Department of Infectious Disease Immunology, Center for Vaccine Research, Statens Serum  
13 Institut, Artillerivej 5, 2300 Copenhagen S, Denmark.

14

15 †These authors contributed equally.

16 \*Corresponding authors

17

18

19 **KEYWORDS:** Self-amplifying RNA, saRNA, RNA vaccines, lipid nanoparticles, polymeric nanoparticles,  
20 solid lipid nanoparticles, route of administration, immunogenicity.

21

22 **Abstract**

23 The efficacy of RNA-based vaccines has been recently demonstrated, leading to the use of mRNA-based  
24 COVID-19 vaccines. The application of self-amplifying mRNA within these formulations may offer further  
25 enhancement to these vaccines, as self-amplifying mRNA replicons enable longer expression kinetics and  
26 more potent immune responses compared to non-amplifying mRNAs. To investigate the impact of  
27 administration route on RNA-vaccine potency, we investigated the immunogenicity of a self-amplifying  
28 mRNA encoding the rabies virus glycoprotein encapsulated in different nanoparticle platforms (solid lipid  
29 nanoparticles (SLNs), polymeric nanoparticles (PNPs) and lipid nanoparticles (LNPs)). These were  
30 administered via three different routes: intramuscular, intradermal and intranasal. Our studies in a mouse  
31 model show that the immunogenicity of our 4 different saRNA vaccine formulations after intramuscular  
32 or intradermal administration was initially comparable; however, ionizable LNPs gave higher long-term  
33 IgG responses. The clearance of all 4 of the nanoparticle formulations from the intramuscular or  
34 intradermal administration site was similar. In contrast, immune responses generated after intranasal was  
35 low and coupled with rapid clearance for the administration site, irrespective of the formulation. These  
36 results demonstrate that both the administration route and delivery system format dictate self-amplifying  
37 RNA vaccine efficacy.

38  
39  
40  
41  
42  
43  
44  
45  
46  
47  
48  
49  
50

## 51 **Introduction**

52 The role of mRNA vaccines in global healthcare is now well established. mRNA vaccines can be classified  
53 into modified and non-modified mRNA and self-amplifying mRNA (saRNA) vaccines. saRNA are developed  
54 from the genome of positive-stranded RNA viruses (usually alphaviruses) in which the genes encoding the  
55 viral structural proteins are replaced by the gene(s) encoding the antigen(s) of interest. They also contain  
56 the alphavirus-based open read frame that encodes four nonstructural proteins (nsP1-4). When  
57 expressed, nsP1-4 form RNA-dependent RNA polymerase (RDRP) complexes, which enables self-  
58 amplification [1]. As a consequence, saRNA replicons enable longer expression kinetics [2] and  
59 significantly more potent immune responses [3] than non-amplifying mRNAs. However, RNAs are  
60 polyanionic and susceptible to enzymatic degradation, limiting their entry into cells, therefore, delivery  
61 systems are needed. Incorporation of RNA vaccines into nanoparticles provides RNA protection and  
62 improved delivery into cells. To date, lipid nanoparticles (LNPs) based on ionizable amino-lipids are the  
63 most advanced RNA delivery systems [4] and this technology is deployed in COVID-19 vaccines [5,6].

64 Previous studies on saRNA-LNPs suggest that the route of administration strongly influences the kinetics  
65 and magnitude of antigen expression as well as the potency of the immune response, though most studies  
66 focus on intramuscular (IM) as the preferred way to deliver both mRNA and saRNA vaccines [7–10]. For  
67 example, Geall and co-workers demonstrated that the intramuscular injection of a saRNA encoding  
68 respiratory syncytial virus fusion protein (RSV-F) either unformulated or formulated within lipid  
69 nanoparticles elicited neutralizing antibody titers in both mice and rats; however, saRNA-LNPs were  
70 significantly more potent than naked saRNA [11]. It has also been reported that LNPs based on either 1,2-  
71 dioleoyl-3-trimethylammonium-propane (DOTAP) or dimethyldioctadecylammonium (DDA) and co-  
72 formulated with saRNA-HIV-1 Env gp140 induced equivalent IgG antibody responses against the target  
73 protein in mice when administered intramuscularly [12]. However, antigen-specific immunity with mRNA  
74 can be achieved via several other administration routes, e.g. intravenous, intradermal (ID), subcutaneous  
75 (SC), intranodal, and intrasplenic [13]. For example, the immunogenicity of a saRNA vaccine encoding the  
76 HIV gp140 surface glycoprotein, formulated in LNPs based on the ionizable lipid DLin-DMA, was tested  
77 after administration by a variety of routes and it was shown to be more effective when administered via  
78 the IM route compared with the ID and SC routes, though the differences between IM and ID groups was  
79 not significant [11]. Similarly, IM or ID vaccination with a hemagglutinin (HA)-encoded saRNA vaccine  
80 formulated in LNPs resulted in comparable antibody and HA inhibition titers [14]. In a third study, also  
81 with an HA-mRNA-LNP vaccine, HAI titers were significantly higher following ID vaccination compared to  
82 IM two weeks after the boost, but equivalent at later time points [15].

83 However, consideration of alternative routes for vaccination may offer opportunities. For example, the  
84 derma skin layer is abundant in professional antigen presenting cells e.g. dendritic dermal cells and  
85 Langerhans cells [16] which can enhance encoded antigen transportation to the lymph nodes and induce  
86 protective immune responses. Thus, intradermal administration may facilitate lower vaccine doses (dose-  
87 sparing) thereby reducing costs (including transport and storage) and expanding the supply chain. Indeed,  
88 the potential of dermal non-viral delivery of saRNA vaccines was reported previously [17]; the skin is  
89 extremely immune competent, easily accessible and drugs can be administered by means of needle-free  
90 devices, thus improving patient compliance, reducing the risk of needle-stick injuries and reducing clinical  
91 waste. Intranasal (IN) vaccination is another needle-free, noninvasive administration route for vaccines.  
92 The nasal cavity is embedded with a high density of dendritic cells that can mediate strong systemic and  
93 local immune responses against pathogens [18]. The uptake of nasally administered vaccines is mediated  
94 by M cells, which can transport particulate antigens to the nasal lymphoid tissue by transcytosis. Nasal  
95 vaccination induces both systemic and mucosal immunity in the respiratory and genital tracts by the  
96 release of IgA into the nasal passage and intestinal tract. This administration route is adopted by  
97 AstraZeneca's FluMist (a live-attenuated influenza virus vaccine approved for human use) and has been  
98 investigated for the delivery of an mRNA-based HIV vaccine, with strong systemic and mucosal anti-HIV  
99 immune responses as well as cytokine productions being achieved [19].

100 Whilst both intradermal and intranasal administration offers potential advantages, there is limited  
101 understanding on RNA vaccine efficacy when given via these routes compared with the conventional  
102 intramuscular route. Therefore, the aim of this study was to compare the efficacy of self-amplifying mRNA  
103 vaccines when delivered using 4 different delivery platforms and via the intramuscular, intradermal or  
104 intranasal route. Building on our previous studies, where we show that lipid nanoparticles (LNPs), solid  
105 lipid nanoparticles (SLNs) and polymeric nanoparticles (PNPs) based on commercially available cationic  
106 lipids such as 1,2-dioleoyl-3-trimethylammonium-propane (DOTAP) efficiently deliver self-amplifying  
107 mRNA vaccines in mice [20,21], we investigate the role of administration route on the immunogenicity  
108 elicited. To compare their performance across different delivery routes, the same formulations were  
109 tested across the different routes. An saRNA encoding the rabies virus glycoprotein (RVG) was used, as  
110 commercial vaccines can be tested as benchmarks and immunological correlates of protection are well-  
111 established [22,23].

112

## 113 **Materials and Methods**

114 **Materials**

115 1,2-dioleoyl-sn-3-phosphoethanolamine (DOPE), dimethyldioctadecylammonium bromide (DDA), 1,2-  
116 dioleoyl-3-trimethylammonium-propane (DOTAP) and 1,2-dimyristoyl-sn-glycero-3-  
117 phosphoethanolamine-N-[methoxy(polyethylene glycol)-2000] (DMG-PEG2000) were obtained from  
118 Avanti Polar Lipids (Alabaster, US). Poly (D, L-lactide-co-glycolide) lactide: glycolide (50:50), MW 30,000-  
119 60,000, Dimethyl Sulfoxide, Tristearin (Grade II-S, ≥90%), 3 M sodium acetate buffer pH 5.2, Trizma  
120 hydrochloride solution 1 M, penicillin-streptomycin, L-glutamine, cholesterol (Chol) and brefeldin A (BFA)  
121 were purchased from Sigma (Milan, Italy). RiboGreen RNA assay kit, 1,1'-Dioctadecyl-3,3,3',3'-  
122 Tetramethylindotricarbocyanine Iodide (DiR), Alexa Fluor 488-labeled goat anti-mouse IgG2a Cross-  
123 Adsorbed secondary antibody and allophycocyanin (APC) Zenon antibody labelling kit for mouse IgG2a  
124 were purchased from Thermo Fisher (Milan, Italy). Dulbecco's Modified Eagle Medium (DMEM), Roswell  
125 Park Memorial Institute 1640 medium (RPMI-1640), Hank's balance salt solution (HBSS) trypsin-EDTA  
126 (0.25%) and fetal bovine serum (FBS) were obtained from Gibco. PLATELIA Rabies II Kit was obtained from  
127 Bio-Rad (Milan, Italy). 100 mM citrate buffer pH 6.0 was purchased from Teknova (Milan, Italy). Live/dead  
128 fixable dead cell stain near-IR was purchased from Life Technologies (Milan, Italy). Mouse anti-rabies  
129 glycoprotein antibody (clone 24-3F-10) was obtained from Merck (Milan, Italy). 10X Perm/Wash buffer  
130 and Cytofix/Cytoperm were obtained from BD Biosciences (San Jose, CA, USA). Anti-mouse PE-CF594-  
131 conjugated CD8, V421-conjugated CD44, PE-conjugated TNF- $\alpha$  and BV786-conjugated IFN- $\gamma$  and FITC-  
132 conjugated CD107a monoclonal antibodies and anti-mouse Ig,  $\kappa$ /negative control compensation particles  
133 set were obtained from BD Horizon (San Jose, CA, USA). Anti-mouse BV510-conjugated CD4, APC-  
134 conjugated CD3 and PE-Cy5-conjugated IL-2 monoclonal antibodies and RBC lysis buffer were purchased  
135 from Biolegend (San Diego, CA, USA). Anti-mouse PE-Cy7-conjugated IL-17, CD28 and CD3 monoclonal  
136 antibodies was purchased from ePharmingen (San Jose, CA, USA). The rabies peptide pool containing  
137 peptides of 15-mers with 11 amino acid overlap were obtained from Genescript (Piscataway NJ, USA).  
138 Rabipur is a trademark of the GSK group of companies.

139 **Synthesis of self-amplifying RNA (saRNA)**

140 A self-amplifying RNA (saRNA) vaccine encoding the rabies virus glycoprotein (RVG) was synthesized as  
141 previously described [11]. In brief, DNA plasmids encoding the RVG-saRNA were constructed using  
142 standard molecular techniques. Plasmids were amplified in Escherichia coli and purified using Qiagen  
143 Plasmid Maxi kits (Qiagen, Germantown, MD, USA). DNA was linearized following the 3' end of saRNA  
144 sequence by restriction digest. Linearized DNA templates were transcribed into RNA using a MEGAscript  
145 T7 kit (Life Technologies, Carlsbad, CA, MA, USA) and purified by LiCl precipitation. RNA was then capped

146 using the Vaccinia Capping system (New England BioLabs, Ipswich, MA, USA) and purified by LiCl  
147 precipitation before formulation.

#### 148 **Formulation and characterization of LNPs, PNPs and SLNs**

149 DOTAP-based formulations were prepared and characterized as previously described [20,21]. In essence,  
150 DOTAP LNPs were composed of DOPE, DOTAP and DMG-PEG2000 at 49:49:2 molar ratio; DOTAP PNPs  
151 were composed of PLGA (lactide:glycolide 50:50) and DOTAP 1:1 w/w and DOTAP-SLNs were composed  
152 of tristearin, DOTAP (1:1 w/w) and 2 mole % of DMG-PEG2000. These formulations were produced by a  
153 microfluidic mixer (Precision NanoSystems Inc., Vancouver, Canada) using a flow rate ratio of 3:1 (for LNPs  
154 and SLNs) or 1:1 (for PNPs) and flow rate of 15 mL/min. Benchmark iLNPs described by Geall et al [11]  
155 were produced in the same manner as cLNPs. Lipids/polymers dissolved in an organic solvent (methanol,  
156 DMSO or ethanol for LNPs, PNPs and SLNs respectively) and an aqueous phase (100 mM citrate buffer pH  
157 6.0 for LNPs, 10 mM TRIS pH 7.4 for SLNs or 100 mM acetate buffer pH 6 for PNPs) containing RVG-saRNA  
158 at 8:1 N:P (N in DOTAP and P in saRNA) were injected simultaneously in the micromixer. All formulations  
159 were dialyzed against 10 mM TRIS pH 7.4 and characterized in terms of hydrodynamic size (Z-average),  
160 polydispersity index (PDI) and zeta potential by dynamic light scattering (DLS) in a Zetasizer Nano ZS  
161 (Malvern, UK) at 0.1 mg/mL at 25 °C. The saRNA encapsulation efficiency (saRNA E.E.) was quantified by  
162 RiboGreen assay following manufacturer instructions. Fluorescence was measured at excitation and  
163 emission wavelength of 485 and 528 nm. saRNA E.E. was calculated as  $(F_T - F_0)/F_T$  where  $F_T$  and  $F_0$  are the  
164 amount of saRNA quantified in presence and absence of 1 % Triton X-100 respectively. Prior to in vivo  
165 administration, formulations were diluted to dosing concentration with the addition of NaCl 20 mM in the  
166 dilution buffer to maintain isotonicity. Low levels of endotoxins (<10 EU/mL) and sterility conditions were  
167 preserved across all formulations.

#### 168 **Immunization studies**

169 All animal studies were ethically reviewed and carried out in accordance with European Directive  
170 2010/63/EEC and the GSK policy on the Care, Welfare and Treatment of Animals. Experiments were  
171 performed at the GSK Animal Facility in Siena, Italy, in compliance with the relevant guidelines (Italian  
172 Legislative Decree n. 26/14) and the institutional policies of GSK. The animal protocol was approved by  
173 the Animal Welfare Body of GSK Vaccines, Siena, Italy, and by the Italian Ministry of Health (Approval  
174 number "AWB 2015 01", CPR/2015/01). Groups of 10 female BALB/c mice (Charles Rivers) aged 6–8 weeks  
175 and weighing about 20–25 g were immunized with RVG-saRNA formulated in either LNPs, PNPs or SLNs  
176 on days 0 and 28 either intramuscularly (IM), intradermally (ID) or intranasally (IN). Mice received 0.15 µg

177 of saRNA-RVG in 50  $\mu$ L when administered IM, 0.15  $\mu$ g of RVG-saRNA in 20  $\mu$ L when administered ID or  
178 1.5  $\mu$ g in 50  $\mu$ L when given IN. Three further groups were vaccinated with the commercial vaccine Rabipur  
179 (a trademark of the GSK group of companies) either IM (2% of the human dose (HD), 50  $\mu$ L), ID (2% HD,  
180 20  $\mu$ L) or IN (5% HD, 50  $\mu$ L). A higher dose was given IN due to the expected reduced efficacy of this route.

### 181 **Quantification of antibody titers**

182 Sera from individual mice were collected four weeks after first vaccination (day 28) and two weeks after  
183 second vaccination (day 42) and combined in five pools of two mice each. Total anti-RVG IgG titers were  
184 quantified with the PLATELIA RABIES II Kit Ad Usum Veterinarium [22] following manufacturer  
185 instructions.

### 186 **Intracellular cytokine staining (ICS) in splenocytes**

187 Spleens from 3 randomly selected mice from each experimental group were collected on day 42 (two  
188 weeks after second vaccination). Single cell suspensions were obtained as described elsewhere [24]. Cells  
189 were then incubated with RBC lysis buffer (2 mL) at 4 °C for 2 minutes, resuspended in complete RPMI  
190 (cRPMI) and passed again through cell strainers. Cells were counted in a Vi-CELL XR cell counter (Beckman  
191 Coulter) and  $1.5 \cdot 10^6$  splenocytes/well were cultured in round-bottomed 96-well plates. Splenocytes were  
192 stimulated with an RVG-derived peptide pool library (2.5  $\mu$ g/mL) consisting on 15-mers with 11 amino  
193 acid overlaps and anti-CD28 (2  $\mu$ g/mL) in presence of brefeldin A (5  $\mu$ g/mL) for 4 hours at 37 °C. Cells were  
194 also stimulated with anti-CD3 (1  $\mu$ g/mL) plus anti-CD28 (2  $\mu$ g/mL) or anti-CD28 alone as positive and  
195 negative controls respectively. Samples were then stained with a live/dead fixable near-IR dead cell stain  
196 kit, then fixed and permeabilized with Cytofix/Cytoperm and subsequently stained with the following  
197 antibodies in Perm/Wash Buffer: APC-conjugated anti-CD3, BV510-conjugated anti-CD4, PE-CF594-  
198 conjugated anti-CD8, BV785-conjugated anti-IFN- $\gamma$ , PE-Cy5-conjugated anti-IL-2, anti-BV605-conjugated  
199 TNF- $\alpha$  and PE-Cy7-conjugated anti-IL-17. Samples were acquired in an LSR II flow cytometer (BD  
200 Biosciences, San Jose, CA, USA) and analyzed in FlowJo Software (BD BioScience, San Jose, CA, USA)).  
201 Antigen-specific CD4+ T cell subsets were identified based on the combination of secreted cytokines as  
202 follows: Th1 (IFN- $\gamma$ + IL-2+ TNF- $\alpha$ +; IFN- $\gamma$ + IL-2+; IFN- $\gamma$ + TNF- $\alpha$ +; IFN- $\gamma$ +); Th0 (IL-2+ TNF- $\alpha$ +; IL-2+; TNF- $\alpha$ +).  
203 The frequency of antigen-specific CD8+ T cells were identified based on the combination of IFN- $\gamma$ +, IL-2+  
204 and TNF- $\alpha$ +

### 205 **Lung processing and quantification of T-cell derived cytokines**

206 Lung tissue was completely dissociated with Gentlemax Dissociator (Milteny Biotec, Bologna, Italy).  
207 Briefly, lung tissue was digested in Hank's Balanced Salt Solution containing calcium and magnesium in



208 presence of collagenase D (2 mg/mL) and DNase I (80 units/mL) (both from Sigma (Milan, Italy)) for 30  
209 min at 37°C, and then homogenized until obtaining a single-cell suspension. Then,  $2 \times 10^6$  cells were seeded  
210 into 96-well U-bottom plates stained with Live/Dead Near InfraRed, fixed and permeabilized, plated with  
211 anti-CD28 mAb (2 µg/mL) and anti-CD107a FITC (5 µg/mL). As positive control, cells were added to wells  
212 coated with anti-CD3 mAb (1 µg/mL). Moreover, as ex vivo restimulation, cells were stimulated for 4 hours  
213 with an RVG peptide pool at 2.5 µg/mL. Brefeldin A (5 µg/mL) was added to each condition for the last 4  
214 hours. For flow cytometry analysis, cells were incubated with anti-CD16/CD32 Fc block and further stained  
215 with anti-CD3-APC, anti-CD4-BV510, anti-CD8 PE, anti-IFN-γ BV785, anti-IL-2 PE-Cy5.5, anti-TNF-α PE,  
216 and anti-CD44 V421, anti-IL-17 PE as intracellular markers. Samples acquisition and analysis were  
217 performed as described above.

### 218 **Biodistribution studies**

219 Biodistribution studies were conducted under the regulations of the Directive 2010/63/EU. All protocols  
220 were subjected to ethical review and were carried out in a designated establishment in the animal facility.  
221 All work was carried out under a project license with approval from the University of Strathclyde Ethical  
222 Review Board. In order to track their biodistribution in vivo, LNPs, PNPs and SLNs were co-formulated with  
223 the lipophilic fluorescent dye 1,1'-Diocetadecyl-3,3,3',3'-Tetramethylindotricarbocyanine Iodide (DiR) as  
224 previously described [25]. Groups of five 6-8-week-old female BALB/c mice injected with either LNPs, PNPs  
225 or SLNs (25 µg, containing 1 µg of DiR dye) intramuscularly (50 µL in the right thigh), intradermally (20 µL  
226 in the dorsum) or intranasally (10 µL per nostril). Mice imaging was carried out using an IVIS Spectrum  
227 (Perkin Elmer, Beaconsfield, UK) using Living Image software for data capture and analysis. The presence  
228 of DiR was detected using an excitation wavelength of 710 nm and an emission filter of 780 nm. A medium  
229 binning and f/stop of 2 was used and acquisition time was determined for each image with auto-exposure  
230 settings. Mice were anaesthetized for imaging using 3% Isoflurane. Anesthesia was maintained during  
231 imaging at 1% Isoflurane. Images were taken before administration of formulations and after 4, 24, 48,  
232 72, 144 and 240 hours post injection. The total flux (p/s) was calculated at the injection site (region of  
233 interest) for each mouse and normalised by dividing each time point by the value at 4 h time point as it  
234 was the highest in each group. This was considered as 100%,

### 235 **Statistical Analysis**

236 Statistical analysis of T cell responses and biodistribution experiments was performed by one-way analysis  
237 of variance (ANOVA) followed Tukey's honest significance test. Statistical analysis of IgG titers was

238 performed by Kruskal-Wallis followed by Dunn's test. P values below 0.05 (\*) were considered significant.  
239 All analyses were done in GraphPad Prism 7.0.

## 240 **RESULTS AND DISCUSSION**

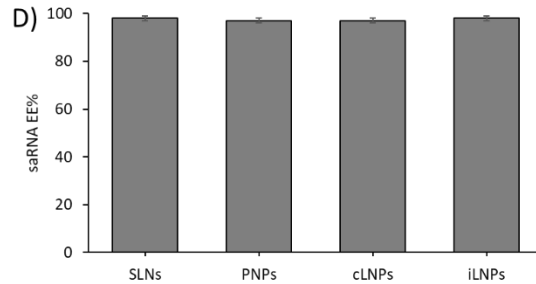
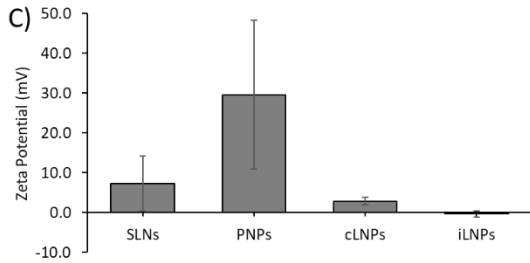
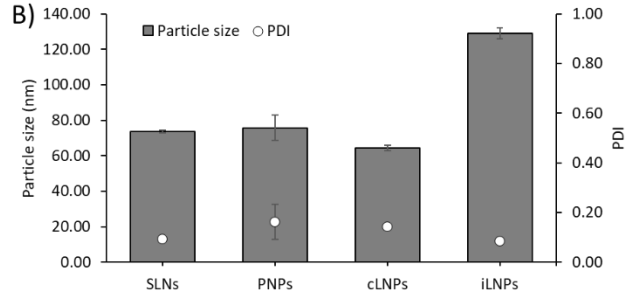
### 241 **Characterization of saRNA-nanoparticles**

242 We have previously reported the microfluidic production of several nanoparticles based on the  
243 commercially available cationic lipid DOTAP [20,21]. The use of microfluidics in the manufacturing process  
244 supports process driven size control and scale-independent production [26,27]. Within this study, we  
245 selected three different nanoparticle formats (LNPs, PNPs and SLNs) to further investigate the role of  
246 administration route on self-amplifying RNA vaccine performance (Figure 1). Whilst cationic LNPs tend to  
247 display bilayer-like structures [28], PNPs consisting of a polymer core and SLNs have a lipid monolayer  
248 surrounding the polymer core [29]. These formulations were selected based on previous studies which  
249 demonstrated these formulations were capable of associating with cells, inducing antigen expression *in*  
250 *vitro* and protecting SaRNA against enzymatic degradation [20,21]. The same formulations were used  
251 across the different delivery routes to allow direct comparison. Our particles were from 65 to 135 nm in  
252 size, with low PDI (<0.2), near neutral zeta potential, except for the PNPs which were cationic in nature,  
253 and high saRNA encapsulation efficiency (>95%) (Figure 1 B-D). Particle size has been suggested to play a  
254 role in the immunogenicity of mRNA vaccines in mice [30]. However more recent studies suggest this may  
255 only be a feature of small animal studies [31]; a retrospective analysis of mRNA LNP vaccine *in vivo* studies  
256 revealed a relationship between LNP particle size and immunogenicity in mice using LNPs of various  
257 compositions. Nevertheless, whilst small diameter LNPs were substantially less immunogenic in mice, all  
258 particle sizes tested yielded a robust immune response in non-human primates [31].

259

A) Nanoparticle Composition

SLNs	DOTAP, tristearin and DMG-PEG2000
PNPs	DOTAP, PLGA and DMG-PEG2000
cLNPs	DOTAP, DOPE and DMG-PEG2000
iLNPs	Ionizable lipid, DOPE and DMG-PEG2000



260  
 261 **Figure 1. Physicochemical characterization of saRNA formulations.** SLNs, PNPs, cLNPs and iLNPs were  
 262 prepared as outlined in (A) and characterized in terms of B) particles size (d.nm) and polydispersity index  
 263 (PDI), C) zeta-potential (mV) and D) encapsulation efficiency (EE%). Results are represented as mean  $\pm$  SD  
 264 of two different batches used for first and second vaccination respectively.  
 265

266 **Immunogenicity of RVG-saRNA formulated in LNPs, PNPs and SLNs following intramuscular, intradermal**  
 267 **and intranasal administration**

268 mRNA and saRNA vaccines are commonly administered IM or ID [16,32] and mRNA vaccines are now  
 269 approved for IM administration. However, there very few pre-clinical studies that have systematically  
 270 compared the immunogenicity of RNA vaccines delivered by different routes of administration. Therefore,  
 271 using the formulations outlined in Figure 1, we assessed the impact of administration route on saRNA  
 272 vaccine efficacy when delivered using the different nanoparticle formats. Mice were vaccinated twice,  
 273 four weeks apart, with RVG-saRNA formulated in either SLNs, PNPs, cLNPs or benchmark iLNPs [33] and  
 274 delivered intramuscularly (IM), intradermally (ID) or intranasally (IN). Control groups were vaccinated with  
 275 or Rabipur, an inactivated rabies virus vaccine. The selected doses were based on our previous findings  
 276 with these delivery systems [20,21] (Table 1).

277  
 278

279

280

281 **Table 1. Routes of administration and vaccine (RVG-saRNA or Rabipur) doses used to immunize BALB/c**  
 282 **mice.** saRNA: self-amplifying RNA; LNPs: lipid nanoparticles, PNPs: polymeric nanoparticles; SLNs: solid-  
 283 lipid nanoparticles; IM: intramuscular; ID: intradermal; IN: intranasal; HD: human dose

Vaccine	Route of administration	Dose	Dose volume
saRNA (formulated in LNPs, PNPs or SLNs)	IM	0.15 µg	50 µL
	ID	0.15 µg	20 µL
	IN	1.5 µg	50 µL
Rabipur	IM	2% HD	50 µL
	ID	2% HD	20 µL
	IN	5% HD	50 µL

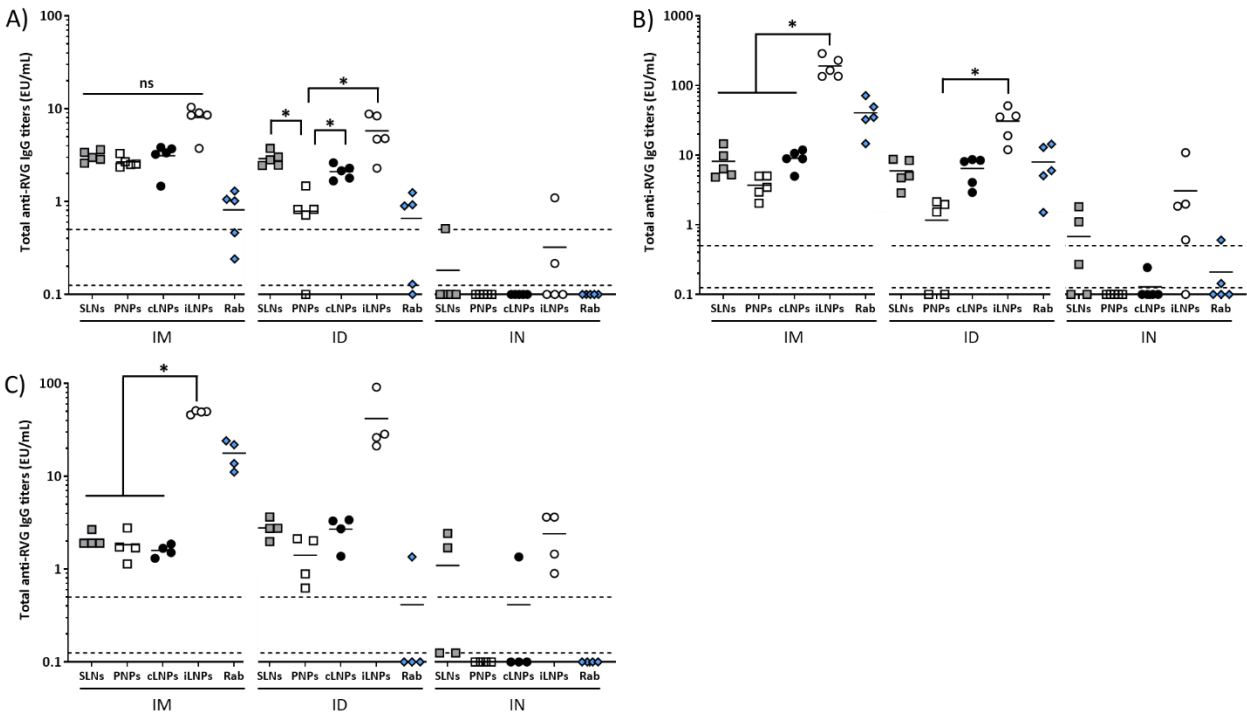
284  
 285 IgG responses were measured, prior to immunization, 4 weeks post first injection (day 28), 2 weeks after  
 286 the second injection (day 42) and 10 weeks after the second injection (day 98). No anti-RVG IgGs were  
 287 detected in mice sera prior to immunization (data not shown). Four weeks after the first injection, there  
 288 was no significant difference between the IgG responses promoted by the 4 different nanoparticle  
 289 formulations (SLNs, PNPs, cLNPs, iLNPs) when administered IM. All 4 nanoparticle formulations induced  
 290 strong antigen-specific IgG titers above the correlate of protection of 0.5 EU/mL and these responses were  
 291 significantly ( $p < 0.05$ ) higher than the control vaccine (Rabipur) (Fig. 2A). When the mice were dosed ID,  
 292 generally a similar response profile was shown with antigen-specific IgG titers above the correlate of  
 293 protection of 0.5 EU/mL. However, PNPs promoted significantly lower responses compared to the SLNs,  
 294 cLNPs and the iLNPs benchmark (Fig. 2A). After IN administration there was no notable IgG responses  
 295 measured, with IgG titers below the limit of quantification in all but three samples, despite mice receiving  
 296 a 10 fold higher dose via this route (Fig. 2A). Overall, at this time point, IM and ID administration with  
 297 the various nanoparticle formulations gave comparable responses, with the exception of PLPs given ID.  
 298 Administration via the IN route failed to induce notable responses irrespective of the formulation.

299 After the second vaccination, the immune responses elicited generally increased approximately 3-fold  
 300 after both IM and ID vaccination with the exception of the PNPs, where the booster dose had little effect  
 301 on the immune response (Fig.2B). Comparing between the nanoparticle formulations, with an IM booster  
 302 injection, iLNPs produced significantly ( $p < 0.05$ ) higher IgG responses compared to the three DOTAP  
 303 formulations (SLNs, PNPs, cLNPs). When a second dose was administered ID, there is no difference  
 304 between SLNs, cLNPs and iLNPs. However, PNPs promoted significantly ( $p < 0.05$ ) lower IgG responses  
 305 compared to iLNPs (Fig. 2B). Again, the immune responses induced upon IN immunization were  
 306 significantly weaker compared to IM or ID immunization for all of the formulations tested with only the

307 iLNPs promoting an average response above the correlate of protection (Fig. 2B). Overall, after the second  
308 immunization, iLNPs administered IM promoted the strongest IgG responses (Fig. 2B).

309 This pattern of immune response was also seen 10 weeks post second immunization, demonstrating the  
310 ability of these nanoparticle formulations to induce persistent humoral immunity above the correlate of  
311 protection (Fig.2C). When administered IM, iLNPs continued to promote significantly ( $p < 0.05$ ) higher IgG  
312 titers compared to the SLNs, PNPs and cLNP formulations. When administered ID, there was no significant  
313 difference between the 4 different nanoparticle formulations but a similar trend of higher responses from  
314 iLNPs was seen (Fig. 2C). Comparing between the routes of administration at this timepoint, IM and ID  
315 gave similar response profiles yet when administered IN, only the iLNPs promoted a notable IgG response  
316 with all responses above the correlate of protection (Fig. 2C).

317 The results in Fig. 2 are in line with recent studies of Blakney and co-workers, who reported equivalent  
318 antibody production in mice vaccinated either IM or ID with saRNA formulated within poly(CBA-co-4-  
319 amino-1-butanol) (ABOL)-based nanoparticles at different doses [34]. Although all formulations elicited  
320 antibodies titers above the level of protective response to rabies vaccination reported by WHO [35], LNPs  
321 and SLNs were generally more potent than PNPs two weeks after the second vaccination, and overall  
322 iLNPs gave the highest long term response via both the IM and ID routes. In our previous studies [20,21],  
323 these formulations did not notably differ in terms of *in vitro* antigen expression nor *in vivo* antibody titers  
324 after IM injection. The combination of nanoparticle formulation and route of administration may result in  
325 different cellular kinetic or pharmacokinetic properties e.g. endosomal disruption potential and/or release  
326 kinetics of saRNA. When administered intranasally, all saRNA-nanoparticle formulations were poorly  
327 immunogenic, despite animals receiving a 10-fold higher dose of RVG-saRNA compared to IM or ID (1.5  
328  $\mu\text{g}$  vs 0.15  $\mu\text{g}$ ). The weak immunogenicity of candidates upon IN vaccination may be due to multiple  
329 factors. For example, rapid clearance from the administration site and/or the acidic, protease-rich and  
330 reductase-rich environment of the mucosae [36] may induce potential loss of activity and functionality of  
331 saRNA.



332

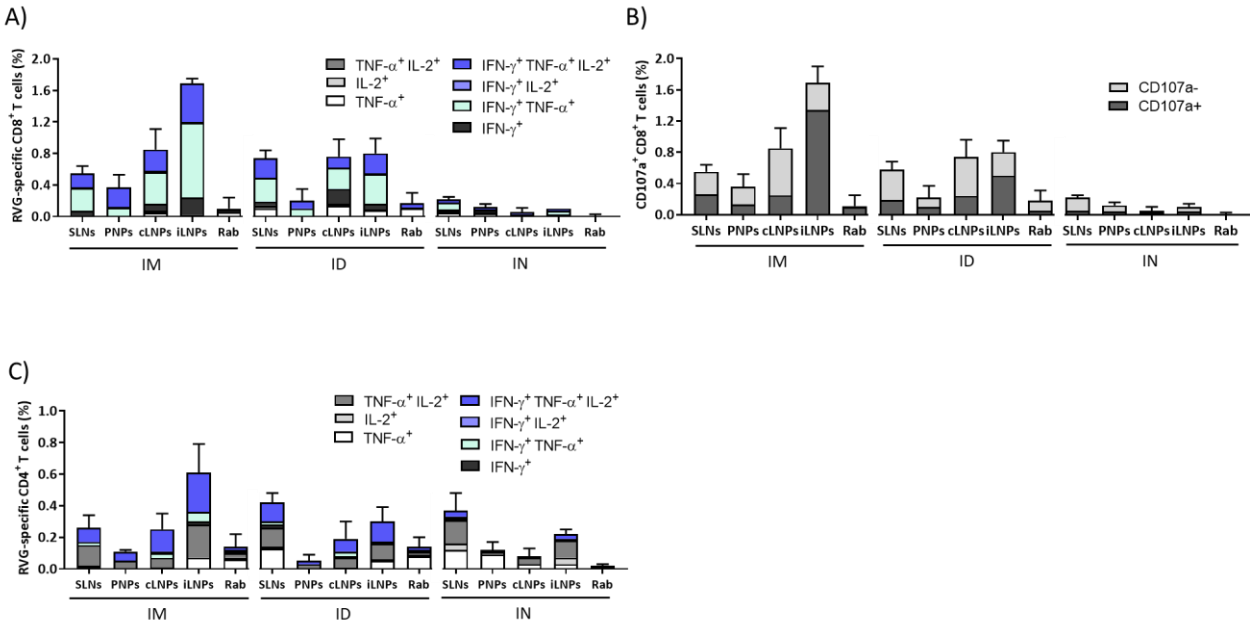
333 **Figure 2. Immunogenicity of RVG-saRNA loaded SLNs, PNPs and LNPs.** Humoral immune responses  
 334 elicited by RVG-saRNA formulated in either DOTAP-based SLNs, PNPs or LNPs following intramuscular (IM,  
 335 0.15  $\mu$ g), intradermal (ID, 0.15  $\mu$ g) or intranasal (IN, 1.5  $\mu$ g) administration in mice. Mice were also  
 336 immunized with benchmark iLNPs [11] or 2% (IM and ID) or 5% (IN) of the human dose of Rabipur. Mice  
 337 were vaccinated four weeks apart and total anti-RVG IgG titers were quantified four weeks after the first  
 338 vaccination (A), two weeks after the second vaccination (B) and 10 weeks after the second vaccination  
 339 (C). Markers depict measurements from pools of 2 mice each. The solid lines represent the geometric  
 340 mean titer of each group (n=4-5). Dotted lines at 0.5 and 0.125 EU/mL correspond to the correlate of  
 341 protection and limit of quantification, respectively.

342

343 To study the immune response profiles further, cytokine responses were also measured. The saRNA-  
 344 nanoparticles formulations induced multifunctional RVG-specific cellular immune responses two weeks  
 345 after the second vaccination (Fig. 3). Generally, LNPs injected either IM or ID induced the highest  
 346 frequencies of cytokines-producing RVG-specific splenic CD4+ and CD8+ T cells (Fig. 3). Similar to the IgG  
 347 profiles, the frequencies of cytokine-producing CD8+ T cells in mice which received iLNPs were greater  
 348 than the other formulations after IM (Fig. 3A). When administered ID, there profiles are similar for the  
 349 SLNs, cLNPs and iLNPs whilst the responses induced by the PNPs are low (Fig. 3A). The majority of RVG-  
 350 specific CD8+ T cells expressed IFN- $\gamma$  in combination with TNF- $\alpha$  and/or IL-2, irrespective of the route of  
 351 administration, and this is generally associated with a mature effector phenotype. The strong proliferation  
 352 of CD8+ T cells triggered by saRNA vaccines is consistent with previous studies which demonstrated that

353 saRNA formulated with LNPs injected IM induced antigen expression within muscle cells and its  
354 consequent presentation to APCs, suggesting cross-priming as the prevalent mechanism for CD8+ T-cell  
355 response activation by saRNA vaccines [37]. Similar to the IgG profiles, the frequencies of cytokine  
356 expression were low in mice vaccinated IN (Fig. 3A). A similar trend was observed in the expression of the  
357 degranulation marker CD107a (Fig. 3B), whose expression correlates with the cytotoxic activity of CD8+ T  
358 cells *in vivo* [38,39]. In mice vaccinated IM, the frequencies of CD107a+ CD8+ T cells were highest with the  
359 iLNPs, whilst after ID, the responses induced by iLNPs reduced and were comparable with the cLNPs and  
360 SLNs (Fig. 3B). After IN administration, only negligible percentages of CD107a+ CD8+ T cells were  
361 quantified (<0.1%, Fig. 3B). With respect to the CD4+ T cell responses, again a similar profile of responses  
362 is seen (Fig. 3C); after IM injection iLNPs promote the highest responses in mice, whilst after ID these  
363 responses reduce and are similar to SLNs and cLNPs (Fig. 3C). However, SLNs administered via the IN route,  
364 promoted responses in line with the responses promoted by SLNs given IM and ID (Fig. 3C).

365 The CD4+ T cells proliferation induced by RNA vaccines is likely to be related to the rapid activation of  
366 lymphatic cells. For example, Liang and colleagues [15] showed that mRNA-LNPs administered either  
367 intradermal or intramuscular in rhesus macaques specifically targeted APCs located both at the injection  
368 site and in draining lymph nodes, leading to antigen translation and upregulation of type I IFN-inducible  
369 genes. This rapid innate immunity induced priming of antigen-specific CD4+ T cells and generation of  
370 vaccine-specific immunity solely in the draining lymph nodes. Similar observations were also reported  
371 elsewhere [40]. The relative frequency of CD8+ and CD4+ T cells quantified for each formulation and route  
372 of administration (Fig. 3) was also consistent with the production of antibodies reported in Fig. 2. A  
373 combination of Th0 (IL-2+/TNF- $\alpha$ +, TNF- $\alpha$ +, or IL-2+) and Th1 (IFN- $\gamma$ + alone or in combination with IL-2+  
374 and/or TNF- $\alpha$ +) phenotypes was observed in CD4+ T-cells 2 weeks after the second immunization in all  
375 groups (Fig. 3C). Interestingly, ID injection of SLNs resulted in the highest frequencies of polyfunctional  
376 antigen-specific CD4+ T cells. The potential of ID vaccination has been widely established in many clinical  
377 trials, although results are not always consistent among different vaccines. For example, dermal injection  
378 of lower doses of a virus-inactivated influenza vaccine resulted in equivalent immunogenicity to the  
379 standard dose delivered intramuscularly [41]. With respect to the rabies virus, post-exposure IM or ID  
380 vaccination with Rabipur resulted in similar neutralizing antibody titers in humans but ID was slightly lower  
381 compared to IM in a pre-exposure prophylaxis regime [42]. Conversely, with hepatitis B vaccine, the  
382 benefit of dose-sparing was not fully evident [43].



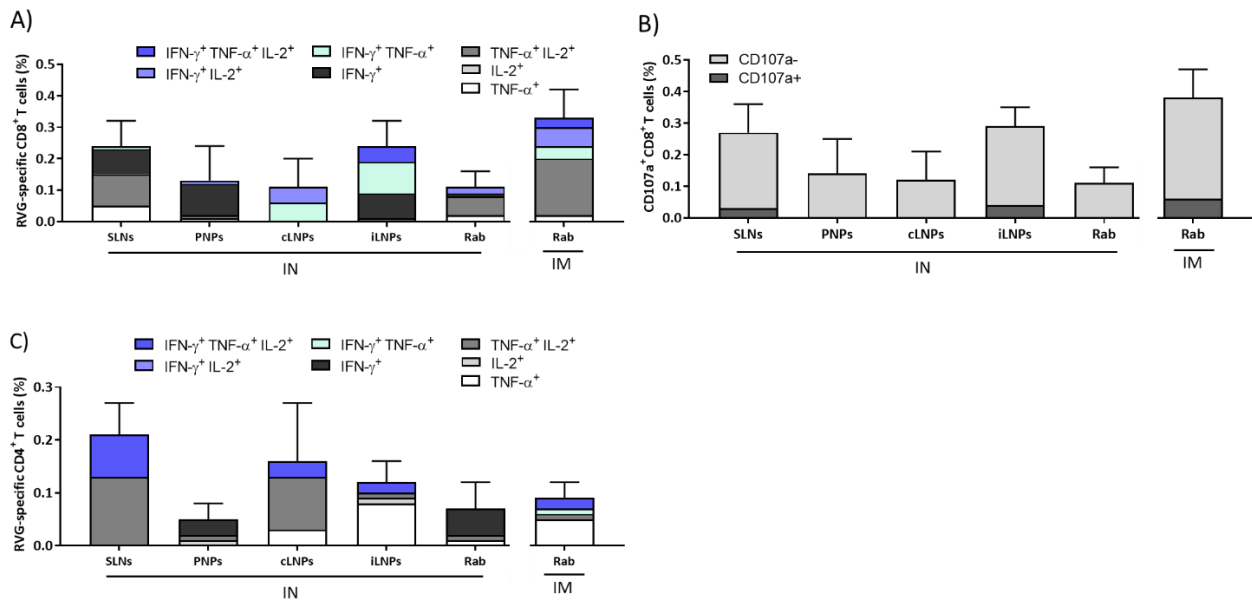
383

384 **Figure 3. Cellular immune response elicited by RVG-saRNA loaded nanoparticles after IM, ID or IN**  
 385 **administration.** Splenic CD8<sup>+</sup> and CD4<sup>+</sup> T cell responses elicited by RVG-saRNA formulated in either  
 386 DOTAP-based SLNs, PNPs and LNPs following intramuscular (IM, 0.15  $\mu$ g), intradermal (ID, 0.15  $\mu$ g) or  
 387 intranasal (IN, 1.5  $\mu$ g) administration in mice. Mice were also immunized with with benchmark iLNPs [11]  
 388 and either 2% (IM and ID) or 5% (IN) of the human dose of Rabipur. Splenocytes were collected two weeks  
 389 after the second vaccination and re-stimulated in vitro with an RVG peptide pool. A) Frequencies of  
 390 cytokine-producing CD8<sup>+</sup> T cells. B) Frequencies of CD107a<sup>+</sup> CD8<sup>+</sup> T cells. C) Frequencies of CD4<sup>+</sup> T cells  
 391 expressed as Th1 and Th0 according to the cytokines expressed. Results are represented as mean  $\pm$  SD of  
 392 three samples. Refer to Figure S1 in the supplemental material for the gating strategy.  
 393

394 Intranasally administered vaccines have the potential to induce persistent lung effector T cells, which  
 395 could significantly benefit host immunity against respiratory pathogens [24]. Therefore, to further  
 396 investigate this, we performed a T cell assay in lung cells from mice immunized IN. iLNPs and SLNs elicited  
 397 higher frequency of RVG-specific CD8<sup>+</sup> T cells compared to LNPs, PNPs and Rabipur when administered  
 398 IN. Furthermore, both formulations gave comparable responses to Rabipur administered IM (Fig. 4A).  
 399 Interestingly, the quality of CD8<sup>+</sup> T cell responses in the lungs varied among tested formulations: SLNs and  
 400 PNPs induced polyfunctional CD8<sup>+</sup> IFN- $\gamma$ <sup>+</sup> and TNF- $\alpha$ <sup>+</sup>/IL-2<sup>+</sup> cells, while those elicited by cLNPs were IFN- $\gamma$   
 401  $\gamma$ /TNF- $\alpha$ <sup>+</sup> and IFN- $\gamma$ <sup>+</sup>/IL-2<sup>+</sup> and those elicited by iLNPs were  $\gamma$ /TNF- $\alpha$ <sup>+</sup>, IFN- $\gamma$ <sup>+</sup>/IL-2<sup>+</sup> and IFN- $\gamma$ <sup>+</sup> (Fig. 4A).  
 402 However, the majority of RVG-specific CD8<sup>+</sup> T-cells were CD107a<sup>-</sup> (Fig. 4B) irrespective of the nanoparticle  
 403 formulation used, which correspond to a non-cytotoxic profile. Regarding CD4<sup>+</sup> T cells, the frequencies of  
 404 RVG-specific cells were comparable between SLNs, cLNPs and iLNPs groups (around 0.2%); however, again  
 405 the profiles were different with the iLNPs promoting more TNF- $\alpha$ <sup>+</sup> cells (Fig. 4C). As observed in splenic



406 CD4+ T-cells, cell profile was a combination of Th0/Th1 phenotypes, with SLNs inducing a higher frequency  
 407 of Th1 cells than LNPs and PNPs respectively (Fig. 4C). These differences in T cell responses may be  
 408 attributed to differences in the nanoparticle chemical composition and/or mRNA delivery profile. For  
 409 example, fatty acids are known to modulate cytokines secretion from activated T cells and the effect is  
 410 dependent on both the saturation degree and length of fatty acid [44,45]. In particular, it was reported  
 411 that saturated fatty acids induced significantly higher release of pro-inflammatory cytokines in T cells than  
 412 their unsaturated counterparts, possibly due to increased formation of free radicals, diacyl glycerol and  
 413 activation of protein kinase C [46].



414  
 415 **Figure 4. Lung CD8<sup>+</sup> and CD4<sup>+</sup> T cell responses following intranasal vaccination.** Lung cells were collected  
 416 two weeks after the second vaccination and re-stimulated in vitro with an RVG peptide pool. A)   
 417 Frequencies of cytokine-producing CD8<sup>+</sup> T cells. B) Frequencies of CD107<sup>+</sup> CD8<sup>+</sup> T cells. C) Frequencies of  
 418 CD4<sup>+</sup> T cells expressed as Th1 and Th0 according to the cytokines expressed. Results are represented as  
 419 mean ± SD of three samples. Refer to Figure S2 in the supplemental material for the gating strategy.  
 420

421 **Biodistribution of saRNA-SLNs, PNPs and LNPs after intramuscular, intradermal and intranasal**  
 422 **administration**

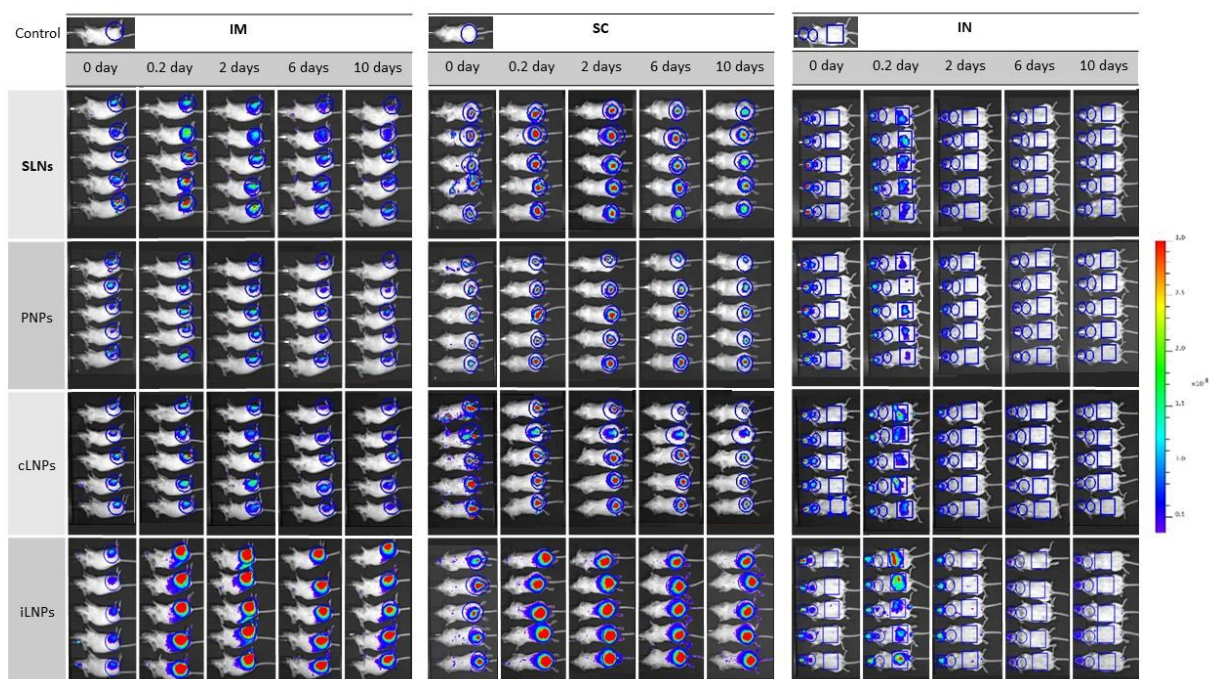
423 Several studies have suggested that the administration route of mRNA vaccines strongly influences the  
 424 kinetics of antigen expression [47]. For example, in a study conducted with mRNA encoding luciferase  
 425 formulated in LNPs, the half-life of antigen expression in mice was ranked in the order of intradermal >>  
 426 intramuscular > intraperitoneal and subcutaneous >> intratracheal > intravenous [47]. Although antigen  
 427 expression, biodistribution and immunogenicity are expected to be closely related, a defined correlation

428 remains unclear. Indeed, we have previously shown that both cLNPs and iLNPs are retained at the injection  
429 site following intramuscular injection for up to 10 days [21]. Here, we compared the pharmacokinetics of  
430 saRNA-SLN, PNPs and LNPs administered via IM, ID or IN in an effort to further understand the  
431 importance of the delivery route for effective mRNA vaccines.

432 When considering the biodistribution of the different nanoparticle formulations (Fig. 5 and 6), full body  
433 images of mice which received saRNA-nanoparticles via intramuscular or intradermal injection showed  
434 that the signal was mainly concentrated at the site of injection (Fig. 5). Long-term retention of all four  
435 nanoparticle formulations at the injection site was also observed after both IM (Fig. 6A) and ID (Fig. 6B)  
436 administration, with the area under the curve (AUC; calculated using the trapezoidal method) confirming  
437 that the drainage profile of the nanoparticles was comparable (Fig. 6D). With respect to IN vaccinated  
438 groups, whole body images showed poor retention of all nanoparticles (Fig. 5); most of the administered  
439 dose was detected in the throat and stomach at 4 hours post administration (Fig. 5) suggesting that part  
440 of the vaccine dose had been rapidly swallowed and cleared a few hours after administration, irrespective  
441 of the nanoparticle format (Fig. 6C and 6D). The rapid clearance of the nanoparticles from the  
442 administration site after IN vaccination correlated with the weaker humoral and cellular immune response  
443 observed. This may result from ineffective interactions between the nanoparticles and mucosal tissue  
444 upon administration due to a lack of muco-adhesive/ muco-penetrating excipients within the nanoparticle  
445 formulations. The presence of muco-adhesive or muco-penetrating polymers (e.g. poly(acrylic acid) (PAA),  
446 alginate, cellulose derivatives, chitosan, poloxamers and poly(ethylene glycol) (PEG)) on the surface of  
447 particles can enhance the concentration of therapeutics delivered to the mucus mesh [48]. Furthermore,  
448 the weak potency of vaccines administered IN may also be linked to the unavoidable limitation of the  
449 animal model used; intranasal vaccination in small animals may trigger inhalation and ingestion of vaccine  
450 antigens, which consequently affects vaccine dosage [49].

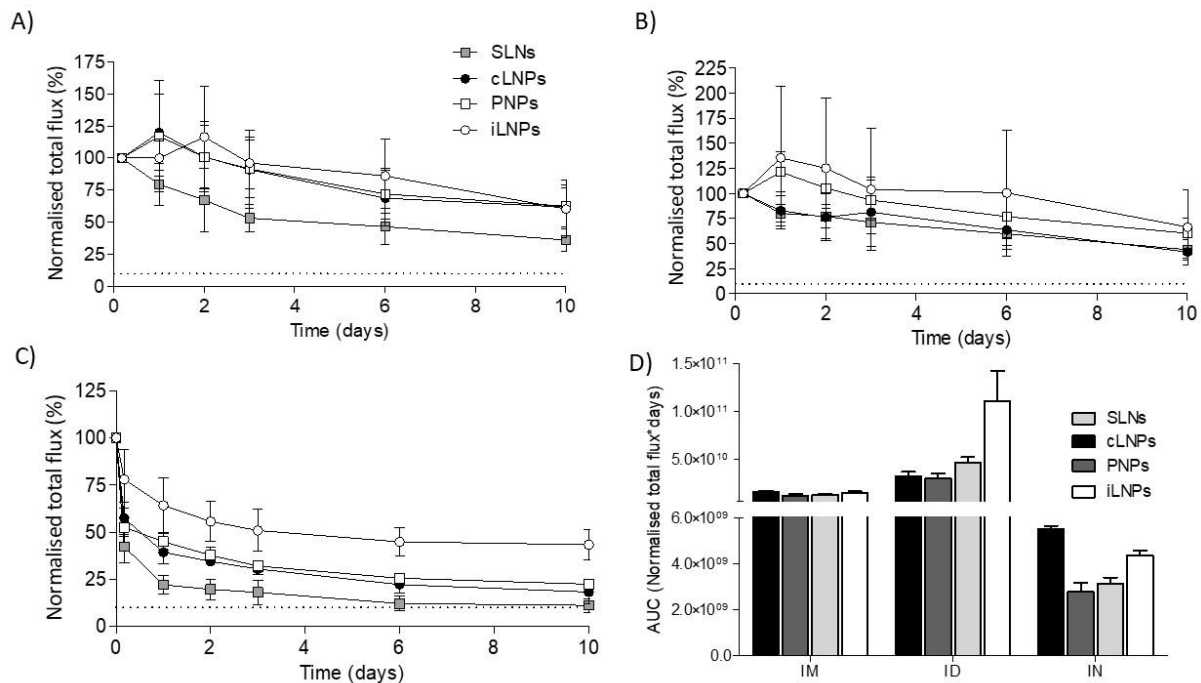
451  
452 By comparing the retention of formulations at the injection site, we did not observe notable differences  
453 in clearance between the four saRNA-nanoparticle formulations from either the IM or ID administration,  
454 despite the formulations inducing different humoral and cellular responses (Fig. 2 and 3). This suggests  
455 that other factors may contribute to the immunogenicity of SaRNA vaccines. These findings are in  
456 agreement with previous investigations which showed poor correlation between pharmacokinetics and  
457 immunogenicity [30]. Accumulation and trafficking of immune cells transporting the encoded antigen to  
458 the draining lymph nodes as well as the mode of antigen delivery to lymphoid tissue might also be involved

459 in the immunostimulatory mechanism of mRNA and saRNA vaccines [40]. The slow clearance of the  
 460 nanoparticles from the injection site could be due to active uptake by host cells via association with  
 461 endogenous ligands (e.g. ApoE) and recognition by scavenger receptors and the low-density lipoprotein  
 462 receptor [50]. ApoE easily associates with the surface of neutral lipid-based particles, resulting in  
 463 enhanced ApoE-mediated cellular uptake [51]. As these receptors are ubiquitously expressed in all  
 464 nucleated cells [52], this active targeting could augment nanoparticle retention at the injection site.



465  
 466 **Figure 5. Biodistribution of RVG-saRNA loaded SLNs, PNPs and LNPs in a mouse model.** Representative  
 467 IVIS images of groups of 5 BALB/c mice injected with either saRNA-SLNs, saRNA-PNPs or saRNA-LNPs by  
 468 the intramuscular (IM), intradermal (ID) or intranasal (IN) route at selected time points. Mice received 25  
 469  $\mu\text{g}$  of nanoparticles, corresponding to the administration of 1  $\mu\text{g}$  of saRNA. The total flux was calculated  
 470 in the regions of interest highlighted in blue. Scale of fluorescence is reported. Refer to Figure S3 in the  
 471 supplementary for enlarged images of mice at all time points over 10 days p.i.

472  
 473  
 474  
 475  
 476  
 477  
 478



479

480 **Figure 6. Pharmacokinetic profile at the site of injection of RVG-saRNA loaded SLNs, PNPs and LNPs.**  
 481 Pharmacokinetic profile at the site of injection of either saRNA-SLNs, saRNA-PNPs or saRNA-LNPs  
 482 following A) intramuscular, B) intradermal or C) intranasal administration. Mice received 25 µg of  
 483 nanoparticles, corresponding to the administration of 1 µg of saRNA. A naive mouse was used as negative  
 484 control. D) Calculated areas under the curve at the site of injection for saRNA encapsulating LNPs, PNPs  
 485 and SLNs administered by intramuscular (IM), intradermal (ID) or intranasal (IN) route. The total flux was  
 486 normalised by dividing each time point by the value at 4 h time point as it was the highest in each group.  
 487 This was considered as 100%. Dotted line represents the background value. Results are represented as  
 488 mean ± SD of five animals per group.

489

## 490 Conclusions

491 In this study, we demonstrate that the immunogenicity of our saRNA vaccines for a given delivery route  
 492 was affected by the format of the nanoparticles. saRNA encapsulated within SLNs and LNPs tending to be  
 493 more potent than PNPs after administration via the intramuscular or intradermal route and immune  
 494 responses from these routes were similar. The clearance of all four saRNA nanoparticle formulations from  
 495 either the IM or ID administration site was also similar. In contrast, immune responses generated after  
 496 intranasal administration was low (despite receiving a 10-fold higher dose) and coupled with rapid  
 497 clearance for the administration site irrespective of the formulation, suggesting that further optimization  
 498 of these systems for this route is required.

499

500

501 **Acknowledgements**

502 We wish to thank the saRNA Vaccine Platform Team at GSK Rockville. We also thank the staff at the Animal  
503 Research Center and at the Flow-Cy-TOF Core Facility at GSK Siena and the Biological Procedures Unit at  
504 University of Strathclyde for technical assistance.

505 **Author Contributions**

506 Conceptualization, G.A., G.L., D.T.O., B.C.B. and Y.P.; methodology G.A., G.L., S.T.S., S.W., C.W.R., S.G.,  
507 M.B., B.C.B. and Y.P.; software, G.A., G.L.; validation, G.A., G.L., S.G., M.B., R.J., B.C.B., S.T.S., S.W. and Y.P.;  
508 formal analysis, G.A. G.L; investigation, G.A. G.L.; resources, G.A., G.L., S.G., M.B., R.J., B.C.B. and Y.P.; data  
509 curation, G.A. G.L.; writing—original draft preparation, G.A. G.L.; writing—review and editing, G.A., G.L.,  
510 S.W., S.T.S., C.W.R., S.G., M.B., R.J., B.C.B. and Y.P.; visualization, Y.P.; supervision, S.G., M.B., R.J., B.C.B.  
511 and Y.P.; project administration, Y.P.; funding acquisition, Y.P. All authors have read and agreed to the  
512 published version of the manuscript.

513 **Funding**

514 This work was funded by the European Commission Project Leveraging Pharmaceutical Sciences and  
515 Structural Biology Training to Develop 21st Century Vaccines (H2020-MSCA-ITN-2015 grant agreement  
516 675370). Independent Research Fund Denmark, grant no. 7026-00027B (STS).

517 **Conflicts of Interest**

518 G.A. and G.L. participated to the European Marie Curie PHA-ST-TRAIN-VAC PhD project at the University  
519 of Strathclyde (Glasgow, UK) in collaboration with GSK (Siena, Italy); the project was co-sponsored  
520 between the University of Strathclyde and GlaxoSmithKline Biologicals S.A. Y.P., S.T.S., C.W.R. and S.W.  
521 declare no conflict of interest. S.G, M.B., R.J., D.T.O. and B.C.B are employees of the GSK group of  
522 companies. All the authors declare that they have no other relevant affiliations or financial interest in  
523 conflict with the subject matter or materials discussed in the manuscript.

524

525 **References**

- 526 [1] C. Iavarone, D.T. O’hagan, D. Yu, N.F. Delahaye, J.B. Ulmer, Mechanism of action of mRNA-based  
 527 vaccines, *Expert Rev. Vaccines*. 16 (2017) 871–881.  
 528 <https://doi.org/10.1080/14760584.2017.1355245>.
- 529 [2] H. Huysmans, Z. Zhong, J. De Temmerman, B.L. Mui, Y.K. Tam, S. Mc Cafferty, A. Gitsels, D.  
 530 Vanrompay, N.N. Sanders, Expression Kinetics and Innate Immune Response after  
 531 Electroporation and LNP-Mediated Delivery of a Self-Amplifying mRNA in the Skin, *Mol. Ther. -*  
 532 *Nucleic Acids*. 17 (2019) 867–878. <https://doi.org/10.1016/j.omtn.2019.08.001>.
- 533 [3] A.B. Vogel, L. Lambert, E. Kinnear, D. Busse, S. Erbar, K.C. Reuter, L. Wicke, M. Perkovic, T.  
 534 Beissert, H. Haas, S.T. Reece, U. Sahin, J.S. Tregoning, Self-Amplifying RNA Vaccines Give  
 535 Equivalent Protection against Influenza to mRNA Vaccines but at Much Lower Doses, *Mol. Ther.*  
 536 26 (2018) 446–455. <https://doi.org/10.1016/j.ymthe.2017.11.017>.
- 537 [4] G. Maruggi, C. Zhang, J. Li, J.B. Ulmer, D. Yu, mRNA as a Transformative Technology for Vaccine  
 538 Development to Control Infectious Diseases, *Mol. Ther.* 27 (2019) 757–772.  
 539 <https://doi.org/10.1016/j.ymthe.2019.01.020>.
- 540 [5] P.F. McKay, K. Hu, A.K. Blakney, K. Samnuan, J.C. Brown, R. Penn, J. Zhou, C.R. Bouton, P. Rogers,  
 541 K. Polra, P.J.C. Lin, C. Barbosa, Y.K. Tam, W.S. Barclay, R.J. Shattock, Self-amplifying RNA SARS-  
 542 CoV-2 lipid nanoparticle vaccine candidate induces high neutralizing antibody titers in mice, *Nat.*  
 543 *Commun.* 11 (2020) 3523. <https://doi.org/10.1038/s41467-020-17409-9>.
- 544 [6] A.K. Blakney, S. Ip, A.J. Geall, An Update on Self-Amplifying mRNA Vaccine Development,  
 545 *Vaccines*. 9 (2021) 97. <https://doi.org/10.3390/vaccines9020097>.
- 546 [7] J. Lutz, S. Lazzaro, M. Habbedine, K.E. Schmidt, P. Baumhof, B.L. Mui, Y.K. Tam, T.D. Madden,  
 547 M.J. Hope, R. Heidenreich, M. Fotin-Mleczek, Unmodified mRNA in LNPs constitutes a  
 548 competitive technology for prophylactic vaccines, *Npj Vaccines*. 2 (2017) 29.  
 549 <https://doi.org/10.1038/s41541-017-0032-6>.
- 550 [8] L.A. Brito, M. Chan, C.A. Shaw, A. Hekele, T. Carsillo, M. Schaefer, J. Archer, A. Seubert, G.R.  
 551 Otten, C.W. Beard, A.K. Dey, A. Lilja, N.M. Valiante, P.W. Mason, C.W. Mandl, S.W. Barnett, P.R.  
 552 Dormitzer, J.B. Ulmer, M. Singh, D.T. O’Hagan, A.J. Geall, A Cationic Nanoemulsion for the  
 553 Delivery of Next-generation RNA Vaccines, *Mol. Ther.* 22 (2014) 2118–2129.  
 554 <https://doi.org/10.1038/mt.2014.133>.
- 555 [9] J.M. Richner, S. Himansu, K.A. Dowd, S.L. Butler, V. Salazar, J.M. Fox, J.G. Julander, W.W. Tang, S.  
 556 Shrestha, T.C. Pierson, G. Ciaramella, M.S. Diamond, Modified mRNA Vaccines Protect against Zika  
 557 Virus Infection, *Cell*. 168 (2017) 1114–1125.e10. <https://doi.org/10.1016/j.cell.2017.02.017>.
- 558 [10] A. Hekele, S. Bertholet, J. Archer, D.G. Gibson, G. Palladino, L.A. Brito, G.R. Otten, M. Brazzoli, S.  
 559 Buccato, A. Bonci, D. Casini, D. Maione, Z.-Q. Qi, J.E. Gill, N.C. Caiazza, J. Urano, B. Hubby, G.F.  
 560 Gao, Y. Shu, E. De Gregorio, C.W. Mandl, P.W. Mason, E.C. Settembre, J.B. Ulmer, J. Craig Venter,  
 561 P.R. Dormitzer, R. Rappuoli, A.J. Geall, Rapidly produced SAM<sup>®</sup> vaccine against H7N9 influenza is  
 562 immunogenic in mice, *Emerg. Microbes Infect.* 2 (2013) 1–7.  
 563 <https://doi.org/10.1038/emi.2013.54>.
- 564 [11] A.J. Geall, A. Verma, G.R. Otten, C.A. Shaw, A. Hekele, K. Banerjee, Y. Cu, C.W. Beard, L.A. Brito, T.  
 565 Krucker, D.T. O’Hagan, M. Singh, P.W. Mason, N.M. Valiante, P.R. Dormitzer, S.W. Barnett, R.

- 566 Rappuoli, J.B. Ulmer, C.W. Mandl, Nonviral delivery of self-amplifying RNA vaccines, *Proc. Natl.*  
567 *Acad. Sci.* 109 (2012) 14604–14609. <https://doi.org/10.1073/pnas.1209367109>.
- 568 [12] A.K. Blakney, P.F. McKay, B.I. Yus, Y. Aldon, R.J. Shattock, Inside out: optimization of lipid  
569 nanoparticle formulations for exterior complexation and in vivo delivery of saRNA, *Gene Ther.* 26  
570 (2019) 363–372. <https://doi.org/10.1038/s41434-019-0095-2>.
- 571 [13] J.B. Ulmer, P.W. Mason, A. Geall, C.W. Mandl, RNA-based vaccines, *Vaccine.* 30 (2012) 4414–  
572 4418. <https://doi.org/10.1016/j.vaccine.2012.04.060>.
- 573 [14] R. Goswami, D. Chatzikleanthous, G. Lou, F. Giusti, A. Bonci, M. Taccone, M. Brazzoli, S. Gallorini,  
574 I. Ferlenghi, F. Berti, D.T. O’Hagan, C. Pergola, B.C. Baudner, R. Adamo, Mannosylation of LNP  
575 Results in Improved Potency for Self-Amplifying RNA (SAM) Vaccines, *ACS Infect. Dis.* 5 (2019)  
576 1546–1558. <https://doi.org/10.1021/acsinfecdis.9b00084>.
- 577 [15] F. Liang, G. Lindgren, A. Lin, E.A. Thompson, S. Ols, J. Röhss, S. John, K. Hassett, O. Yuzhakov, K.  
578 Bahl, L.A. Brito, H. Salter, G. Ciaramella, K. Loré, Efficient Targeting and Activation of Antigen-  
579 Presenting Cells In Vivo after Modified mRNA Vaccine Administration in Rhesus Macaques, *Mol.*  
580 *Ther.* 25 (2017) 2635–2647. <https://doi.org/10.1016/j.ymthe.2017.08.006>.
- 581 [16] N. Pardi, M.J. Hogan, F.W. Porter, D. Weissman, mRNA vaccines — a new era in vaccinology, *Nat.*  
582 *Rev. Drug Discov.* 17 (2018) 261–279. <https://doi.org/10.1038/nrd.2017.243>.
- 583 [17] A. Selmi, F. Vascotto, K. Kautz-Neu, Ö. Türeci, U. Sahin, E. von Stebut, M. Diken, S. Kreiter, Uptake  
584 of synthetic naked RNA by skin-resident dendritic cells via macropinocytosis allows antigen  
585 expression and induction of T-cell responses in mice, *Cancer Immunol. Immunother.* 65 (2016)  
586 1075–1083. <https://doi.org/10.1007/s00262-016-1869-7>.
- 587 [18] S. Gallorini, D.T. O’Hagan, B.C. Baudner, Concepts in Mucosal Immunity and Mucosal Vaccines, in:  
588 *Mucosal Deliv. Biopharm.*, Springer US, Boston, MA, 2014: pp. 3–33.  
589 [https://doi.org/10.1007/978-1-4614-9524-6\\_1](https://doi.org/10.1007/978-1-4614-9524-6_1).
- 590 [19] M. Li, M. Zhao, Y. Fu, Y. Li, T. Gong, Z. Zhang, X. Sun, Enhanced intranasal delivery of mRNA  
591 vaccine by overcoming the nasal epithelial barrier via intra- and paracellular pathways, *J. Control.*  
592 *Release.* 228 (2016) 9–19. <https://doi.org/10.1016/j.jconrel.2016.02.043>.
- 593 [20] G. Anderluzzi, G. Lou, S. Gallorini, M. Brazzoli, R. Johnson, D.T. O’Hagan, B.C. Baudner, Y. Perrie,  
594 Investigating the Impact of Delivery System Design on the Efficacy of Self-Amplifying RNA  
595 Vaccines, *Vaccines.* 8 (2020) 212. <https://doi.org/10.3390/vaccines8020212>.
- 596 [21] G. Lou, G. Anderluzzi, S.T. Schmidt, S. Woods, S. Gallorini, M. Brazzoli, F. Giusti, I. Ferlenghi, R.N.  
597 Johnson, C.W. Roberts, D.T. O’Hagan, B.C. Baudner, Y. Perrie, Delivery of self-amplifying mRNA  
598 vaccines by cationic lipid nanoparticles: The impact of cationic lipid selection, *J. Control. Release.*  
599 325 (2020) 370–379. <https://doi.org/10.1016/j.jconrel.2020.06.027>.
- 600 [22] M. Feysaguet, L. Dacheux, L. Audry, A. Compoin, J.L. Morize, I. Blanchard, H. Bourhy,  
601 Multicenter comparative study of a new ELISA, PLATELIA™ RABIES II, for the detection and  
602 titration of anti-rabies glycoprotein antibodies and comparison with the rapid fluorescent focus  
603 inhibition test (RFFIT) on human samples from vaccinated and non-vacc, *Vaccine.* 25 (2007)  
604 2244–2251. <https://doi.org/10.1016/j.vaccine.2006.12.012>.
- 605 [23] L. Stantj -Pavlinj, M., Hostnik, P., Levinik-Stežinar, S., Zaletel-Kragelj, Vaccination against rabies  
606 and protective antibodies - comparison of ELISA and fluorescent antibody virus neutralization

- 607 (FAVN) assays, *Vet. Arh.* 76 (2006) 281–289.
- 608 [24] S. Gallorini, M. Taccone, A. Bonci, F. Nardelli, D. Casini, A. Bonificio, S. Kommareddy, S. Bertholet,  
609 D.T. O’Hagan, B.C. Baudner, Sublingual immunization with a subunit influenza vaccine elicits  
610 comparable systemic immune response as intramuscular immunization, but also induces local IgA  
611 and TH17 responses, *Vaccine.* 32 (2014) 2382–2388.  
612 <https://doi.org/10.1016/j.vaccine.2013.12.043>.
- 613 [25] D. Chatzikleanthous, S.T. Schmidt, G. Buffi, I. Paciello, R. Cunliffe, F. Carboni, M.R. Romano, D.T.  
614 O’Hagan, U. D’Oro, S. Woods, C.W. Roberts, Y. Perrie, R. Adamo, Design of a novel vaccine  
615 nanotechnology-based delivery system comprising CpGODN-protein conjugate anchored to  
616 liposomes, *J. Control. Release.* 323 (2020) 125–137.  
617 <https://doi.org/10.1016/j.jconrel.2020.04.001>.
- 618 [26] C.B. Roces, G. Lou, N. Jain, S. Abraham, A. Thomas, G.W. Halbert, Y. Perrie, Manufacturing  
619 Considerations for the Development of Lipid Nanoparticles Using Microfluidics, *Pharmaceutics.*  
620 12 (2020) 1095. <https://doi.org/10.3390/pharmaceutics12111095>.
- 621 [27] G. Anderluzzi, S.T. Schmidt, R. Cunliffe, S. Woods, C.W. Roberts, D. Veggi, I. Ferlenghi, D.T.  
622 O’Hagan, B.C. Baudner, Y. Perrie, Rational design of adjuvants for subunit vaccines: The format of  
623 cationic adjuvants affects the induction of antigen-specific antibody responses, *J. Control.*  
624 *Release.* 330 (2021) 933–944. <https://doi.org/10.1016/j.jconrel.2020.10.066>.
- 625 [28] J.A. Kulkarni, M.M. Darjuan, J.E. Mercer, S. Chen, R. Van Der Meel, J.L. Thewalt, Y.Y.C. Tam, P.R.  
626 Cullis, On the Formation and Morphology of Lipid Nanoparticles Containing Ionizable Cationic  
627 Lipids and siRNA, *ACS Nano.* 12 (2018) 4787–4795. <https://doi.org/10.1021/acs.nano.8b01516>.
- 628 [29] J. Ghitman, E.I. Biru, R. Stan, H. Iovu, Review of hybrid PLGA nanoparticles: Future of smart drug  
629 delivery and theranostics medicine, *Mater. Des.* 193 (2020) 108805.  
630 <https://doi.org/10.1016/j.matdes.2020.108805>.
- 631 [30] K.J. Hassett, K.E. Benenato, E. Jacquinet, A. Lee, A. Woods, O. Yuzhakov, S. Himansu, J. Deterling,  
632 B.M. Geilich, T. Ketova, C. Mihai, A. Lynn, I. McFadyen, M.J. Moore, J.J. Senn, M.G. Stanton, Ö.  
633 Almarsson, G. Ciaramella, L.A. Brito, Optimization of Lipid Nanoparticles for Intramuscular  
634 Administration of mRNA Vaccines, *Mol. Ther. - Nucleic Acids.* 15 (2019) 1–11.  
635 <https://doi.org/10.1016/j.omtn.2019.01.013>.
- 636 [31] K.J. Hassett, J. Higgins, A. Woods, B. Levy, Y. Xia, C.J. Hsiao, E. Acosta, Ö. Almarsson, M.J. Moore,  
637 L.A. Brito, Impact of lipid nanoparticle size on mRNA vaccine immunogenicity, *J. Control. Release.*  
638 335 (2021) 237–246. <https://doi.org/10.1016/j.jconrel.2021.05.021>.
- 639 [32] P.S. Kowalski, A. Rudra, L. Miao, D.G. Anderson, Delivering the Messenger: Advances in  
640 Technologies for Therapeutic mRNA Delivery, *Mol. Ther.* 27 (2019) 710–728.  
641 <https://doi.org/10.1016/j.ymthe.2019.02.012>.
- 642 [33] P.R. Cullis, M.J. Hope, Lipid Nanoparticle Systems for Enabling Gene Therapies, *Mol. Ther.* 25  
643 (2017) 1467–1475. <https://doi.org/10.1016/j.ymthe.2017.03.013>.
- 644 [34] A.K. Blakney, Y. Zhu, P.F. McKay, C.R. Bouton, J. Yeow, J. Tang, K. Hu, K. Samnuan, C.L. Grigsby,  
645 R.J. Shattock, M.M. Stevens, Big Is Beautiful: Enhanced siRNA Delivery and Immunogenicity by a  
646 Higher Molecular Weight, Bioreducible, Cationic Polymer, *ACS Nano.* 14 (2020) 5711–5727.  
647 <https://doi.org/10.1021/acs.nano.0c00326>.



- 648 [35] S.A. Plotkin, Vaccines: Correlates of Vaccine-Induced Immunity, *Clin. Infect. Dis.* 47 (2008) 401–  
649 409. <https://doi.org/10.1086/589862>.
- 650 [36] V. Bourganis, O. Kammona, A. Alexopoulos, C. Kiparissides, Recent advances in carrier mediated  
651 nose-to-brain delivery of pharmaceuticals, *Eur. J. Pharm. Biopharm.* 128 (2018) 337–362.  
652 <https://doi.org/10.1016/j.ejpb.2018.05.009>.
- 653 [37] S. Lazzaro, C. Giovani, S. Mangiavacchi, D. Magini, D. Maione, B. Baudner, A.J. Geall, E. De  
654 Gregorio, U. D’Oro, C. Buonsanti, CD8 T-cell priming upon mRNA vaccination is restricted to  
655 bone-marrow-derived antigen-presenting cells and may involve antigen transfer from myocytes,  
656 *Immunology.* 146 (2015) 312–326. <https://doi.org/10.1111/imm.12505>.
- 657 [38] L. Zaritskaya, M.R. Shurin, T.J. Sayers, A.M. Malyguine, New flow cytometric assays for  
658 monitoring cell-mediated cytotoxicity, *Expert Rev. Vaccines.* 9 (2010) 601–616.  
659 <https://doi.org/10.1586/erv.10.49>.
- 660 [39] E. Aktas, U.C. Kucuksezer, S. Bilgic, G. Erten, G. Deniz, Relationship between CD107a expression  
661 and cytotoxic activity, *Cell. Immunol.* 254 (2009) 149–154.  
662 <https://doi.org/10.1016/j.cellimm.2008.08.007>.
- 663 [40] K.E. Lindsay, S.M. Bhosle, C. Zurla, J. Beyersdorf, K.A. Rogers, D. Vanover, P. Xiao, M. Araínga,  
664 L.M. Shirreff, B. Pitard, P. Baumhof, F. Villinger, P.J. Santangelo, Visualization of early events in  
665 mRNA vaccine delivery in non-human primates via PET–CT and near-infrared imaging, *Nat.*  
666 *Biomed. Eng.* 3 (2019) 371–380. <https://doi.org/10.1038/s41551-019-0378-3>.
- 667 [41] G. Icardi, A. Orsi, A. Ceravolo, F. Ansaldi, Current evidence on intradermal influenza vaccines  
668 administered by Soluvia™ licensed micro injection system, *Hum. Vaccin. Immunother.* 8 (2012)  
669 67–75. <https://doi.org/10.4161/hv.8.1.18419>.
- 670 [42] A. Giesen, D. Gniel, C. Malerczyk, 30 years of rabies vaccination with Rabipur: a summary of  
671 clinical data and global experience, *Expert Rev. Vaccines.* 14 (2015) 351–367.  
672 <https://doi.org/10.1586/14760584.2015.1011134>.
- 673 [43] Y. Levin, E. Kochba, I. Hung, R. Kenney, Intradermal vaccination using the novel microneedle  
674 device MicronJet600: Past, present, and future, *Hum. Vaccin. Immunother.* 11 (2015) 991–997.  
675 <https://doi.org/10.1080/21645515.2015.1010871>.
- 676 [44] A.J. de Jong, M. Kloppenburg, R.E.M. Toes, A. Ioan-Facsinay, Fatty Acids, Lipid Mediators, and T-  
677 Cell Function, *Front. Immunol.* 5 (2014). <https://doi.org/10.3389/fimmu.2014.00483>.
- 678 [45] U. Radzikowska, A.O. Rinaldi, Z. Çelebi Sözüner, D. Karaguzel, M. Wojcik, K. Cypryk, M. Akdis, C.A.  
679 Akdis, M. Sokolowska, The Influence of Dietary Fatty Acids on Immune Responses, *Nutrients.* 11  
680 (2019) 2990. <https://doi.org/10.3390/nu11122990>.
- 681 [46] F.B. Stentz, A.E. Kitabchi, Palmitic acid-induced activation of human T-lymphocytes and aortic  
682 endothelial cells with production of insulin receptors, reactive oxygen species, cytokines, and  
683 lipid peroxidation, *Biochem. Biophys. Res. Commun.* 346 (2006) 721–726.  
684 <https://doi.org/10.1016/j.bbrc.2006.05.159>.
- 685 [47] N. Pardi, S. Tuyishime, H. Muramatsu, K. Kariko, B.L. Mui, Y.K. Tam, T.D. Madden, M.J. Hope, D.  
686 Weissman, Expression kinetics of nucleoside-modified mRNA delivered in lipid nanoparticles to  
687 mice by various routes, *J. Control. Release.* 217 (2015) 345–351.  
688 <https://doi.org/10.1016/j.jconrel.2015.08.007>.

- 689 [48] K. Netsomboon, A. Bernkop-Schnürch, Mucoadhesive vs. mucopenetrating particulate drug  
690 delivery, *Eur. J. Pharm. Biopharm.* 98 (2016) 76–89. <https://doi.org/10.1016/j.ejpb.2015.11.003>.
- 691 [49] V. Gerdtts, S. van D. Littel-van den Hurk, P.J. Griebel, L.A. Babiuk, Use of animal models in the  
692 development of human vaccines, *Future Microbiol.* 2 (2007) 667–675.  
693 <https://doi.org/10.2217/17460913.2.6.667>.
- 694 [50] A. Akinc, W. Querbes, S. De, J. Qin, M. Frank-Kamenetsky, K.N. Jayaprakash, M. Jayaraman, K.G.  
695 Rajeev, W.L. Cantley, J.R. Dorkin, J.S. Butler, L. Qin, T. Racie, A. Sprague, E. Fava, A. Zeigerer, M.J.  
696 Hope, M. Zerial, D.W. Sah, K. Fitzgerald, M.A. Tracy, M. Manoharan, V. Koteliansky, A. de  
697 Fougères, M.A. Maier, Targeted Delivery of RNAi Therapeutics With Endogenous and  
698 Exogenous Ligand-Based Mechanisms, *Mol. Ther.* 18 (2010) 1357–1364.  
699 <https://doi.org/10.1038/mt.2010.85>.
- 700 [51] Y. Suzuki, H. Ishihara, Structure, activity and uptake mechanism of siRNA-lipid nanoparticles with  
701 an asymmetric ionizable lipid, *Int. J. Pharm.* 510 (2016) 350–358.  
702 <https://doi.org/10.1016/j.ijpharm.2016.06.124>.
- 703 [52] J.L. Goldstein, M.S. Brown, The LDL Receptor, *Arterioscler. Thromb. Vasc. Biol.* 29 (2009) 431–  
704 438. <https://doi.org/10.1161/ATVBAHA.108.179564>.
- 705